Journal of Geochemical Exploration 282 (2026) 107961

Contents lists available at ScienceDirect

Journal of Geochemical Exploration

journal homepage: www.elsevier.com/locate/gexplo

Portable X-ray fluorescence (pXRF) application to the determination of major and trace elements in large soil datasets for geochemical background assessment

Iker Martínez-del-Pozo [a,*], Mónica Celina Gómez-Pachón [a], Inmaculada Ferri-Moreno [a], Mari Luz García-Lorenzo [a], Saturnino Lorenzo [b], José Ignacio Barquero-Peralbo [b], Xabier Arroyo [c], Pablo Higueras [b], José María Esbrí [a]

[a] Departamento de Mineralogía y Petrología, Facultad de Ciencias Geológicas, Universidad Complutense de Madrid, Madrid, Spain
[b] Instituto de Geología Aplicada, Universidad de Castilla-La Mancha, Almadén, Spain
[c] Unidad de Técnicas Geológicas, CAI de Ciencias de la Tierra y Arqueometría, Universidad Complutense de Madrid, Spain

ARTICLE INFO

Keywords:
Portable X-ray fluorescence (pXRF)
Geochemistry
Geochemical background
Trace elements
Spatial distribution
Cuenca province (Castilla-La Mancha)

ABSTRACT

Regional soil geochemical surveys are essential for land-use planning and human health. However, projects involving large sample sets characterised using traditional laboratory techniques are costly, time-consuming and require a large number of reagents. Therefore, the use of portable X-ray fluorescence (pXRF) with an optimised measurement time and methodology, along with minimal sample preparation, allows for fast and effective measurements. In this study, using Soil-Fundamental Parameters (S-FP) method, a measurement time of 45 s and low sample preparation yielded acceptable results for K, Ca, Ti, Cr, Mn, Fe, Ni, Cu, Zn, As, Rb, Sr, Zr, and Pb, which were monitored with benchtop XRF equipment. The application of this methodology in Cuenca province, Spain, and the comparison with different European and national programmes provides consistency in the results, despite using different analytical techniques. It was observed that a systematic and regular sampling strategy avoids geochemical gaps, increasing the representativeness of the soil parent material in the samples. Distinct geochemical patterns have been identified, with a major group comprising Ti, Mn and Fe, and trace elements such as Cr, Ni, Cu, Zn, As, Rb, Sr, Zr and Pb, while K, Ca and Sr display individual distribution trends. Therefore, this study provides a rapid and economical way to characterise soil geochemistry in large areas and to establish background and reference levels over extensive regions.

1. Introduction

The concept of establishing a geochemical background (GB) for the Earth's surface emerged following the Chernobyl nuclear accident in 1986, which highlighted the need to geochemically characterise the European surface on a continental scale (Bölviken et al., 1996). This vulnerability initiated the development of large-scale programmes such as Forum of European Geological Surveys (FOREGS), followed by Geochemical Mapping of Agricultural and Grazing land soil (GEMAS), and the systematic soil monitoring initiative under the Land Use/Cover Area frame Survey (LUCAS) programme. FOREGS included over 1600 topsoil samples from 26 European countries (Salminen et al., 1998); GEMAS characterised Ap (agricultural soils) and Gr (grazing soils) samples with 2211 and 2118 samples, respectively, from 33 countries (Reimann et al., 2011; Reimann et al., 2009); while LUCAS currently covers over 20,000 samples from 27 European countries (Tóth et al., 2016; Tóth et al., 2013). These programmes have been fundamental in estimating reference elemental concentrations and generating essential information for environmental management, resource exploration and regulatory policy (Gałuszka and Migaszewski, 2011; Reimann and Garrett, 2005). However, their low sample density limits the analysis of local pollution sources, the assessment of the risk posed by potentially toxic elements (PTEs), and the coverage of regional and local scale conditions (Bednářová et al., 2016). For this reason, higher-resolution national initiatives have been developed, such as the Geochemical Atlas of Spain, which analyses the geochemical distribution of approximately 14,000 topsoil samples, providing a detailed view of geochemical variability at regional and local scales (Locutura Rupérez et al.,

* Corresponding author at: Departamento de Mineralogía y Petrología, Facultad de Ciencias Geológicas, Universidad Complutense de Madrid, Madrid, Spain.
E-mail address: ikerma01@ucm.es (I. Martínez-del-Pozo).

https://doi.org/10.1016/j.gexplo.2025.107961
Received 30 June 2025; Received in revised form 3 December 2025; Accepted 15 December 2025
Available online 18 December 2025

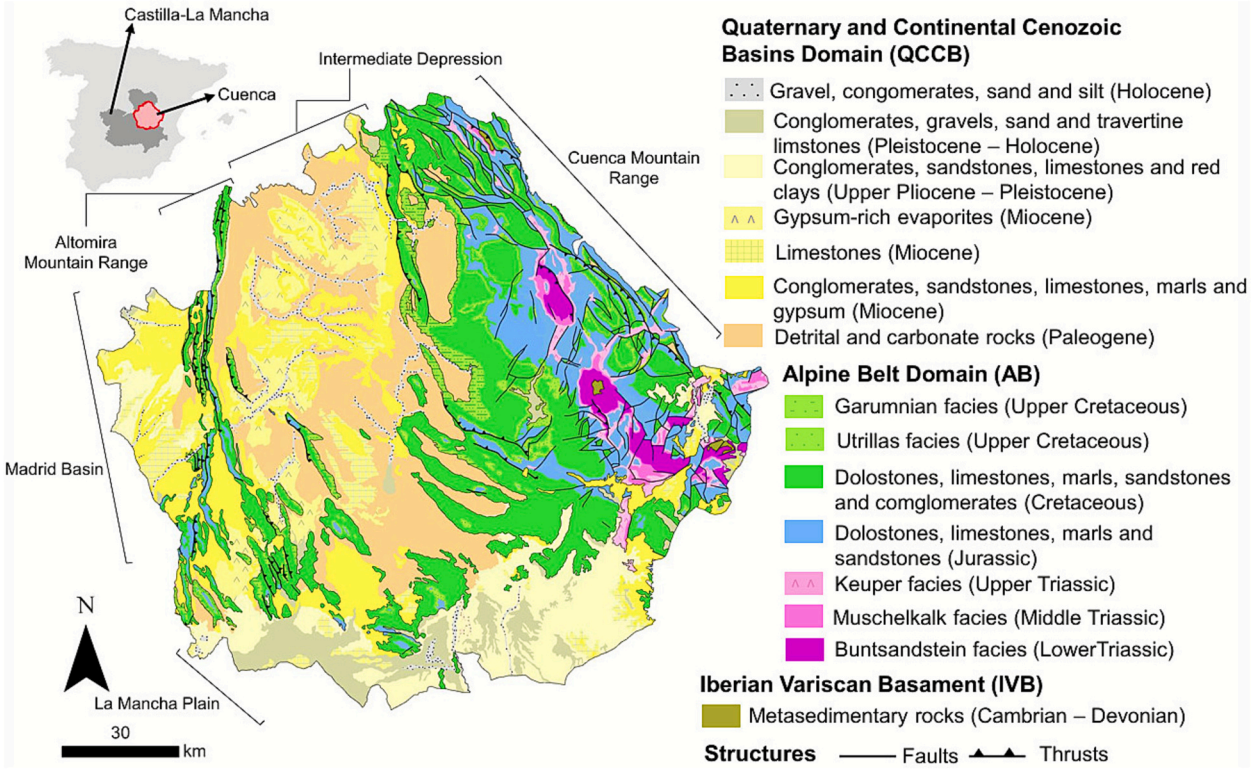

Fig. 1. Simplified geological map of the Cuenca province.
(Modified after Rodríguez Fernández et al., 2015).

2012). High-density, multi-element geochemical campaigns are an essential strategy for establishing geochemical background levels, as they allow elemental variability to be correlated with geological, edaphic, and environmental factors (Cheng et al., 2014; Yuan et al., 2013). However, until now, these studies have largely depended on conventional laboratory analytical techniques, which are expensive, time-consuming, and generate waste.

In contrast, portable X-ray fluorescence spectrometer (pXRF) has achieved an important role in geochemical studies due to its time-saving, non-destructive, low-cost, and versatile nature, aligning with the principles of green chemistry (Horta et al., 2015; Weindorf et al., 2014; Lemière, 2018; Anastas and Warner, 2000). It is essential to acknowledge the technical limitations of pXRF in soil analysis, which are determined by factors such as measurement time, calibration method, moisture content, organic matter content, homogeneity, humidity, particle size, and sample preparation (Li et al., 2022). Proper sample preparation is required to optimise the sensitivity, reliability and elemental detection of the pXRF equipment (Williams et al., 2020). For instance, some authors dry the samples to mitigate the disturbance caused by moisture content, as it absorbs the X-rays and disperses the primary radiation, resulting in poor detection of light elements (Haschke et al., 2021). Milling is also performed to reduce air attenuation and optimise the analysis (Borges et al., 2020; Goff et al., 2020; Zhou et al., 2024). Greater accuracy is also achieved by pressing the samples (with or without the application of additives like cellulose or wax) to obtain greater agglutination and homogeneity of the samples, allowing for more uniform density and smoother surfaces (Haschke et al., 2021; Goff et al., 2020; Byers et al., 2016). Despite these advances, no universally accepted protocol for soil preparation in pXRF analysis currently exists.

Nevertheless, numerous studies have demonstrated that pXRF provides results comparable to conventional analytical methods, which has facilitated its broader implementation in various fields (Sapkota et al., 2019; Silva et al., 2020; Silva et al., 2021). Recent literature shows a significant increase in pXRF applications, but most studies have focused on mineral deposit exploration, lithological discrimination, weathering processes and regolith geochemistry, specific contamination assessments or methodological validations (Ross et al., 2024; Yuan et al., 2021; Bustos et al., 2022; McNulty et al., 2018; Kazimoto et al., 2018). Despite this, there is still limited evidence that pXRF has been applied extensively as the primary technique for building large-volume, regional resolution soil databases explicitly aimed at defining geochemical background.

This methodological and scale gap justifies the critical evaluation of the applicability of pXRF for the definition of regional geochemical background and baseline. For example, in Spain, certain Autonomous Communities could benefit from the absence of GBs. The current absence of these data is largely attributable to administrative delays in conducting these studies, despite their legal responsibility for implementation under Royal Decree 9/2005 (Gobierno de España, 2005). Furthermore, these regions could integrate initiatives supported by the European Regional Development Fund (ERDF), which aims to reduce territorial disparities through technological innovation and the sustainable management of environmental resources (European Commission, 2024). In addition to reinforcing analytical capacity within Europe, these efforts could also support countries with limited infrastructure, thereby contributing to the achievement of the Sustainable Development Goals (SDGs) outlined in the 2030 Agenda and promoting analytical capacity in various geographical contexts (United Nations, 2015). This approach could help existing challenges in developing countries, particularly in remote areas where the use of high-purity gas cylinders for expensive analytical equipment is logistically complex. The methodology proposed in this study could contribute to defining GB, almost simultaneously with sampling, avoiding the need to transport samples to centralized analytical facilities.

In this context, the main objective of this study is to propose a cost-effective methodology for the geochemical analysis of large soil sample sets at regional scale using pXRF. The specific objectives are:

1. To optimise the pXRF measurement parameters and evaluate the matrix effects for different sample preparation methods.
2. To evaluate the representativeness of soil samples in Cuenca province (Castilla La Mancha, Spain) in comparison with national and European datasets.
3. To generate geochemical distribution maps and provide reference information to support the establishment of GB and their application in environmental management.

2. Geological features of the study area

Within the administrative boundaries of the Cuenca province, three geological domains can be recognised, resulting from the superposition of different orogenic and sedimentary episodes. The oldest rocks in the region outcrop in the eastern part of Cuenca province, in the Cuenca Mountain Range, within the Iberian Variscan Basement (IVB) domain (Fig. 1), and are composed of metasedimentary rocks (slate, schist and quartzite) from the Cambrian-Devonian period, forming part of the Variscan basement (Sopeña et al., 2004). This domain is not represented in the sampling conducted in this study, considering it constitutes 0.15 % of the area of Cuenca province.

The Alpine Range domain is represented by the Cordillera Ibérica (IC) in the Cuenca Mountain Range, in the east of the province and the Altomira Mountain Range forming part of the westernmost sector of the IC. The Altomira Mountain Range is comprised of Cretaceous outcrops in a narrow belt of NW-SE folds and thrusts configured in a thin-skinned structural model (Sopeña et al., 2004). This structural model is continued in the Cuenca Mountain Range, which is composed of Permo-Triassic sedimentary rocks forming the Tegument and the Jurassic-Cretaceous overlying materials, where carbonates are the dominant lithologies in the territory. The Triassic evaporitic materials, composing the Keuper Facies, which outcrop in the Cuenca Mountain Range as a detachment level, are particularly noteworthy. The geological complexity of this domain was simplified into three lithological groups in this study: group 1 (G1), predominantly composed of carbonates, including limestones and dolomites, with some marl from Jurassic and Cretaceous periods; group 2 (G2), detrital rocks corresponding to the Triassic Buntsandstein facies and the Cretaceous Utrillas facies; group 3 (G3), gypsiferous rocks associated with the Triassic Keuper facies.

The Cenozoic-Quaternary setting is the most modern domain in Cuenca province, which is subdivided into two small basins. The intracratonic Madrid Basin is located to the west, and a smaller piggy-back basin, known as the Loranca Basin or Intermediate Depression, is situated to the east (Alonso-Zarza et al., 2004).This individualisation of the Tajo Basin developed during the Upper Paleogene upon the uplift of the Altomira Montain Range (Alonso-Zarza et al., 2004). To the south, the domain is constituted by the La Mancha Plain, consisting of the Júcar and Cabriel basins. The post-orogenic sedimentary basins of this domain, which are of Miocene and Plio-Quaternary age, exhibit a wide variety of facies changes, ranging from detrital to carbonate and evaporitic rocks. The continental gypsum units of the Cenozoic, present in this domain, cover a large area in the eastern Iberian Peninsula (Escavy et al., 2012). Located in the Madrid sub-basin, these deposits are concentrated in Paleogene and Neogene sequences and in lacustrine deposits of Miocene sulphates (Calvo et al., 1996). In the Loranca sub-basin, evaporite sedimentation occurred during the late Oligocene to

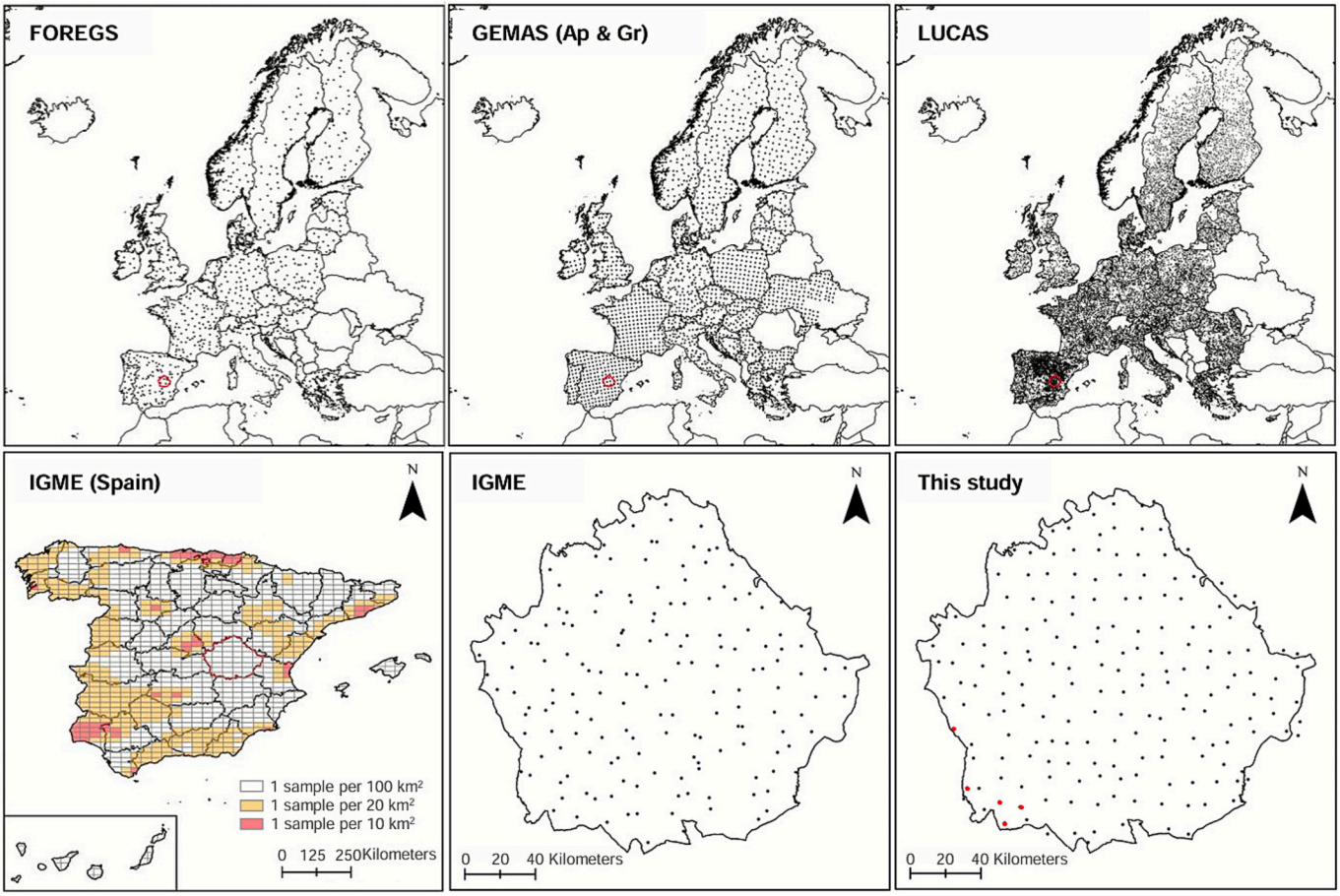

Fig. 2. Distribution maps of samples from different European (FOREGS, GEMAS and LUCAS), national (IGME) programmes in Spain. The figure shows the location of Cuenca province and the sampling sites carried out in this study. The samples highlighted in red are those used for evaluating the influence of samples preparation (matrix effect verification). (For interpretation of the references to colour in this figure legend, the reader is referred to the web version of this article.)

Table 1
Comparison of soil geochemical campaigns of different European and national programmes. Notation: A = A horizon; Ap = Agricultural soil; Gr = Grazing land soil; XRF = X ray fluorescence; ICP-MS = Inductively Coupled Plasma Mass Spectrometry; ICP-AES = Inductively Couple Plasma Atomic Emission Spectroscopy; INAA = Instrumental Neutron Activation Analysis; pXRF = Portable X-ray fluorescence.

Survey	FOREGS	GEMAS		IGME			SCLM
Sample type	A 0–25 cm	Ap 0–20 cm	Gr 0–10 cm	2–20 cm			2–20 cm
Samples	846	2113	2024	907			907
Sample density	1/4700 km^2	1/2500 km^2		1/100 km^2	1/20 km^2	1/10 km^2	1/100 km^2
Sample strategy	Systematic based on drainage basins and lithology	Systematic based on agricultural/grazing uses		Stratified random sampling on drainage network.			Regular systematic based on lithology.
Soil type	Undisturbed, natural light agricultural areas. Colluvial and Alluvial parent soils were avoided	Ap: agricultural Ap-horizon soil (regularly ploughed fields) Gr: grazing land soil (land under permanent grass cover		Non-polluted areas. Colluvial and alluvial parent soils were avoided			Non-polluted areas. Colluvial and alluvial parent soils were avoided
Sample preparation	Dried at 40 °C, sieved to <2 mm and fragmented to <0.063 mm	Dried at room temperature and sieved to <2 mm		Dried at room temperature and sieved <2 mm			Dried at room temperature and prepared with different degrees of processing
Method	XRF (K, Ca, Ti, Cr, Mn, Fe, Zn, Rb, Sr y Zr) Total extraction ICP-MS (Cu, As y Pb)	XRF (all elements)		Total extraction for ICP-MS (Cr, Ni, Cu, Zn, Rb, Sr and Pb) ICP-AES (K, Ca, Ti, Mn and Zr) INAA (Fe and As*)			pXRF (all elements)

* As data not available in shapefile format.

Miocene (Arribas and Díaz-Molina, 1996). This domain is classified into three lithological groups: group 4 (G4), limestone dominated rocks with detrital materials from the Miocene to pre-Pleistocene; group 5 (G5), predominantly detrital rocks containing limestones and gypsum from the Miocene to Holocene; and group 6 (G6), gypsiferous deposits from the Paleogene to Neogene.

3. Material and methods

3.1. Sampling and Project

The Soil sampling campaign of Castilla-La Mancha (SCLM) programme was conducted during 2018–2022. A total of 907 samples were collected from Castilla-La Mancha by the Instituto de Geología Aplicada (UCLM). Topsoil samples were collected from non-anthropogenic and agricultural areas with no recent activity. Soils developed on colluvial, and alluvial deposits were avoided. The sampling strategy was systematically regular, employing a 10 × 10 km grid, with a density of 1 soil sample per 100 km^2. The location of the samples in each cell has been chosen to ensure the representativeness of main lithologies. In 2020, the project was halted because of the high economic costs of the sample treatment and analysis, with only 16 % of the samples being analysed. The sampling campaign for Cuenca province was completed by a second researcher team (UCM), resulting in a total of 210 samples for the present study.

Samples were collected using an Ejkelkamp soil sampler and a metal shovel and were placed in polyethylene bags. In each sampling point, a composite sample was obtained, comprising three subsamples collected at the vertices of a triangle, with a separation distance of 1 m between each subsample. Each subsample was taken from the surface layer of the A horizon (2–20 cm depth), after removing the vegetation cover from the surface O-horizon. The three subsamples were mixed and homogenised to obtain a composite sample of approximately 1–2 kg. To prevent cross-contamination, all sampling tools were washed with deionised water between sites. Subsequently, the samples were dried at room temperature, and a representative and homogeneous aliquot was obtained via quartering. Finaly, samples were analysed with pXRF equipment following the verification control in the following sections.

3.2. Optimisation of pXRF

The pXRF analyses were conducted with a Hitachi X-Met8000 Expert equipment. This portable instrument is equipped with a 40 kV X-ray tube with an Rh tube and a silicon detector. Measurements were made with hands-free with an X-ray security capsule which was controlled by a computer. The elements considered have been Mg, Al, Si, P, S, Cl, K, Ca, Sc, Ti, V, Cr, Mn, Fe, Co, Ni, Cu, Zn, As, Se, Rb, Sr, Zr, Nb, Mo, Cd, Sn, Sb, Ba, Ta, Hg, Tl, Pb, Bi, Th and U.

Multi-element characterization was performed using the pXRF calibrations based on the equipment's fundamental parameter (FP) method, applying corrections for generic matrix effects and optimal energy ranges for the quantification of major, minor, trace elements (Fedeli et al., 2024). However, a quality verification was performed with the Mining Light Element – FP (MLE-FP) and Soil – FP (S-FP) calibration methods with five certified reference materials (CRM): two soils (SO-1 and SO-2) and three sediments (STSP-2, STSP-3 and STSP-4), with two measurement time of 45 s and 90 s. A time of 45 s was the period recommended by the manufacturer. In these verifications and optimisation of measurement times, five replicates were performed for each method and duration. The average concentration of the standard samples was compared with the certified value reported by Plotts et al., 1992, to obtain the mean recovery percentage (MRP) and the correlation coefficient (R^2) to evaluate the accuracy and consistency of the pXRF instrument analyses.

The detection limits provided by the manufacturer for this technique are only indicative, since they depend greatly on the matrix. Consequently, their inclusion in the manuscript has been omitted to avoid errors in data interpretation.

3.3. Optimisation of sample preparation

The study of the effect of sample preparation on pXRF analysis was conducted by selecting five soil samples from the Cuenca province (Fig. 2). For each sample, ex situ preparations with varying degrees of treatment were performed The sample protocol for each type of sample was established individually. P1 samples were dried in a clean plastic bag for several days in the laboratory at room temperature, then

Table 2
LODs of different analytical techniques used by the FOREGS, GEMAS and IGME programmes, and pXRF spectrometer for elements reported in this study in mg kg^{-1}.

Elements	FOREGS		GEMAS	IGME			SCLM
	XRF	ICP-MS	XRF	ICP-MS	ICP-OES	INAA	pXRF
K	100.00*	–	50.00*	–	0.01	–	253.50
Ca	100.00*	–	50.00*	–	0.01	–	155.00
Ti	10.00*	–	10.00*	–	0.01	–	10.00
Cr	3.00	–	4.00	1.00	–	–	1.50
Mn	10.00	–	10.00*	–	1.00	–	50.00
Fe	100.00*	–	3.00	–	–	0.01	175.00
Ni	2.00	–	3.00	1.00	–	–	7.50
Cu	–	0.01	5.00	0.20	–	–	5.00
Zn	3.00	–	3.00	0.20	–	–	2.50
Rb	2.00	–	2.00	0.20	–	–	1.50
As	–	0.20	3.00	–	–	0.50	0.50
Sr	2.00	–	2.00	0.20	–	–	5.00
Zr	3.00	–	3.00	–	2.00	–	1.50
Pb	–	3.00	3.00	1.00	–	–	1.50

* As oxides for FOREGS and GEMAS XRF analyses.

manually homogenised and analysed with the pXRF. Subsequently, portions of P1 were subjected to quartering and sieved to 2 mm mesh size to obtain P2 samples, which were placed in a plastic bag until pXRF analysis. An aliquot of P2 was ground in a mortar and sieved through a 125 μm mesh to obtain P3 samples, which were stored for pXRF analysis. Finally, 9.2 g of P3 was mixed with 0.8 g of wax, pressed at 10 tons for 10 min to obtain a pellet, P4 sample, and analysed with the portable and benchtop XRF. For each sample, three measurements were taken at different spots on the material, and the mean of these replicates was considered as the representative value. Furthermore, the P4 samples were subjected to benchtop XRF analysis using the Bruker S2 Ranger instrument equipped with Pd tube at the Unidad de Técnicas Geológicas (Centro de Asistencia a la Investigación, Ciencias de la Tierra y Arqueometría) of the Universidad Complutense de Madrid. The data obtained from this secondary analysis were considered the reference values (R). The analysis time was approximately 10 min. Elemental analysis was performed using Soils and Sediments method. The concentration range of the samples analysed for each type of sample preparation was compared using boxplots against the reference analysis (R). This approach provides an examination of variability, trends, and potential biases.

3.4. Comparison with European and national datasets

Continental-scale maps, while having a low sampling density, provide essential large-scale context and information on general geochemical trends (de Caritat et al., 2018). Programmes such as FOREGS and GEMAS (at a continental scale) and the Instituto Geológico y Minero de España (IGME) (at a national scale) offer a fundamental benchmark for assessing the coherence and robustness of geochemical patterns found in our study area. This comparison shows whether our analytical method offers the necessary robustness for its application and recommendation for regional geochemical characterization. To this end, the accessible databases from these programmes were downloaded and compared with our data for the Cuenca province, acknowledging the inherent differences in their sampling, soil type, sample preparation, analytical methodology, limit of detection (LOD) values (Table 1 and Table 2). Furthermore, boxplot analyses were employed for this comparison, as it effectively enhances the interpretation of the spatial distribution presented in the geochemical maps (Reimann and Filzmoser, 2000).

3.5. Data processing and spatial analysis

The analytical data were processed using ArcGIS Pro 3.4.0 (ESRI). A spatial database of the sampling points was created for subsequent spatial analysis. Following pXRF optimisation K, Ca, Ti, Cr, Mn, Fe, Ni, Cu, Zn, Rb, As, Sr, Zr and Pb were selected, along with the available elements from the IGME programme for comparative purposes.

Table 3
Descriptive values of CRM concentrations, MRP, recovery range, and recovery coefficient of elements measured by pXRF, compared with their reference values, using the MLE-FP and S-FP methods at 45 s and 90 s measurement times. The results are based on the average of five CRMs, each measured in five replicates.

	Soil 45 s		Soil 90s		Mining 45 s		Mining 90s	
	M RP	R^2	M RP	R^2	M RP	R^2	M RP	R^2
Mg	–	–	–	–	134.7	0.98	130.1	0.98
Al	–	–	–	–	111.0	0.78	111.1	0.77
Si	–	–	–	–	112.7	0.17	112.9	0.17
P	–	–	–	–	145.0	0.99	144.5	0.98
K	101.7	0.98	101.6	0.98	102.4	0.86	102.6	0.86
Ca	103.1	0.93	102.9	0.92	98.5	0.74	98.6	0.74
Ti	104.8	0.99	105.4	0.99	83.5	0.98	82.9	0.97
V	63.4	0.91	54.7	0.95	–	–	–	–
Cr	86.0	0.98	86.8	0.95	–	–	–	–
Mn	107.4	0.99	106.4	1.00	111.5	1.00	108.6	0.99
Fe	109.7	0.89	109.7	0.89	108.2	0.42	108.5	0.42
Co	60.7	0.58	126.3	0.30	175.1	0.25	61.9	0.65
Ni	111.4	0.93	131.2	0.99	107.8	0.99	80.9	0.88
Cu	104.0	0.78	101.7	0.86	92.4	0.48	84.9	0.40
Zn	98.0	0.95	97.5	0.95	101.2	0.77	101.5	0.80
As*	95.3	0.99	96.7	1.00	103.6	0.93	103.4	0.91
Rb	116.2	0.97	114.4	0.96	116.4	0.86	117.1	0.85
Sr	113.1	0.90	112.9	0.89	112.7	0.43	113.4	0.44
Zr	107.8	1.00	107.2	1.00	104.5	0.99	107.0	0.99
Mo	88.9	0.98	112.2	0.94	–	–	–	–
Sn	1824.3	0.13	–	–	–	–	–	–
Sb	931.4	0.29	–	–	–	–	–	–
Ba	102.4	0.99	99.8	0.99	72.0	0.95	69.3	0.96
Ta	3047.1	0.18	2907.2	0.25	2815.4	0.18	2652.6	0.25
Pb	119.1	0.96	116.3	0.96	131.2	0.91	135.0	0.91
Th	126.3	0.96	118.4	0.96	110.9	0.98	113.1	0.94
U	108.2	0.95	85.9	0.98	–	–	–	–

* As was verified using only three CRMs because SO-1 and SO-2 contain low As concentrations.

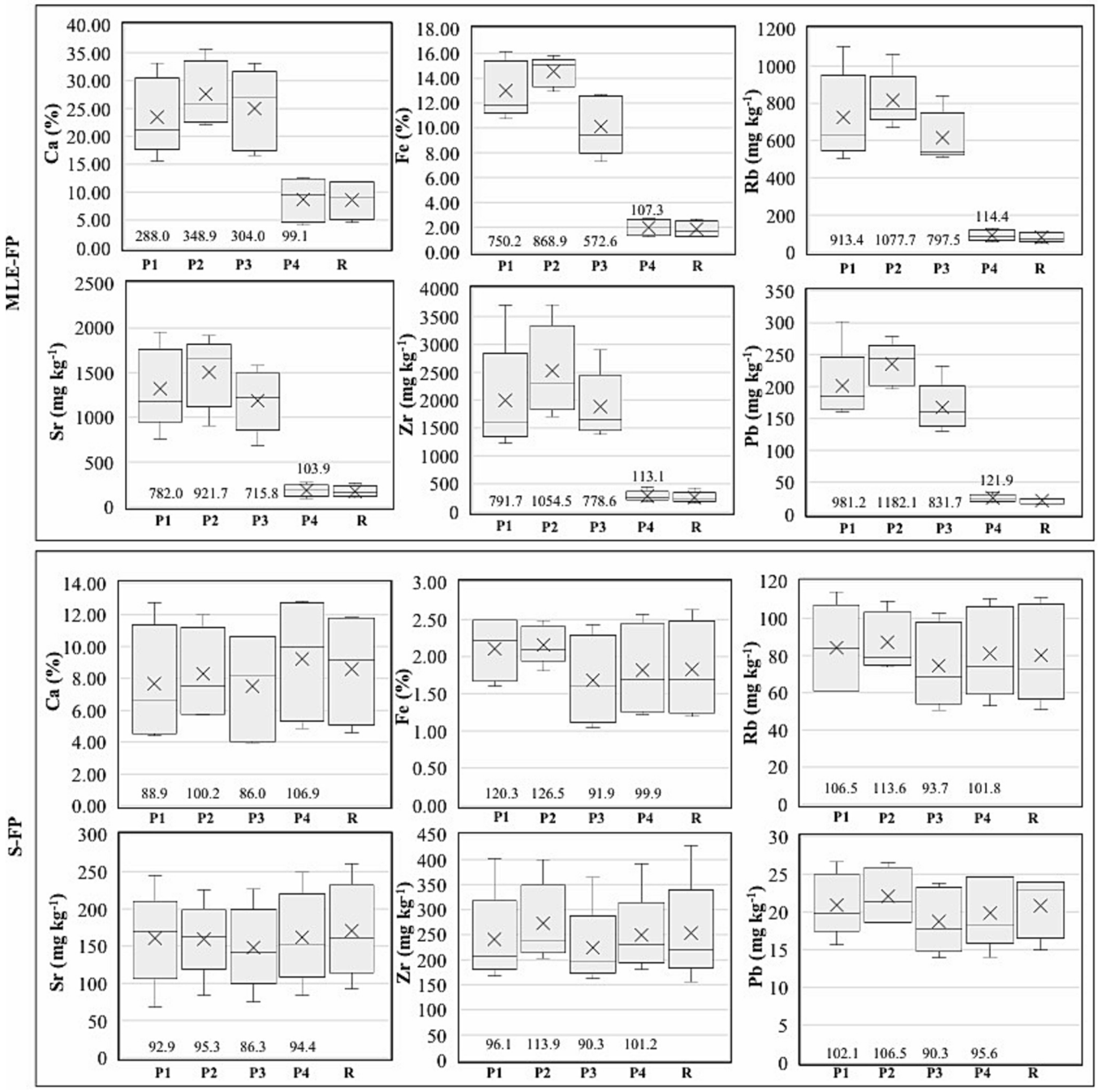

Fig. 3. Boxplots of the concentration of Ca, Fe, Rb, Sr, Zr, and Pb-presented as examples-for the four types of sample preparation (P1–P4) of the five samples analysed. Each preparation type includes three replicates per sample. pXRF results are evaluated against the reference boxplot (R) generated from benchtop XRF measurements. The remaining elements are presented in Fig. S1 and S2. The figure also includes the average Recovery Percentage (RP) for each preparation type with respect to the reference boxplot (R).

Geochemical maps were generated using the same interpolation criteria and threshold as applied in the IGME programme, employing Inverse Distance Weighted (IDW) geostatistical method (Locutura Rupérez et al., 2012). The interpolation was enhanced by including a series of samples located outside the province of Cuenca province boundary. Symbology includes a total of eight colour zones, determined by using the following percentiles: 5 %, 20 %, 30 %, 50 %, 70 %, 80 %, 98 %. The geochemical maps (SCLM and IGME) presented the percentiles calculated from the internal Cuenca province, except for As, for which IGME percentiles were used. The ETRS 1989 – UTM Zone 30 N XY coordinate system was employed.

The representativeness index (RI) was calculated to provide a simplified evaluation of the correspondence between the soil parental material and the distribution of soil samples. First, the area occupied by each assigned lithological group (section 2) was quantified at a 1:1,000,000 scale, discarding small, unrepresented lithological polygons. These quantified areas were then normalized to 100 %. Subsequently, the percentage of samples assigned to each lithological group was calculated. The RI was defined as the ratio between the percentage of samples and the percentage of area each lithological group. An RI of 1 implies proportional representativeness, an RI < 1, indicates underrepresentation, and RI > 1 indicates overrepresentation. This index was

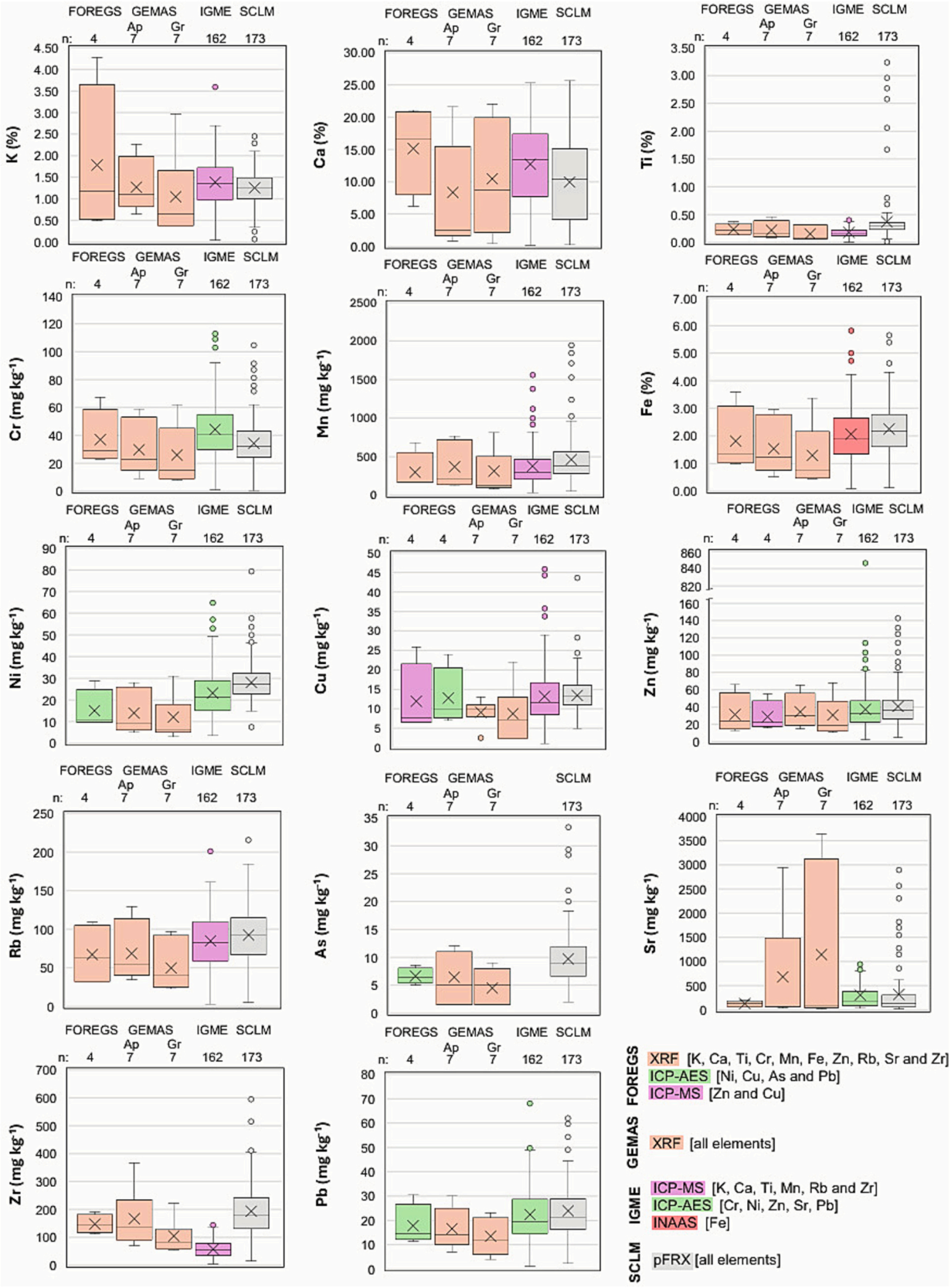

Fig. 4. Comparative boxplot of each element analysed in SCLM study against the different programmes, FOREGS, GEMAS and IGME, for samples located in Cuenca province.

applied to both the IGME and SCLM data. All surface area calculations were performed using ArcGIS Pro. The geological maps used for the classification of the geology of Cuenca province were sourced from the 1:1,000,000 scale Geological Map of Spain (Rodríguez Fernández et al., 2015).

In this technique, limit of detection (LOD) may vary depending on the tube and detector and the geometry of the analyser, as well as the composition of the sample matrix (Lemière, 2018) . In this work, the elements with concentrations above LOD are K (100 %), Ca (100 %), Ti (100 %), Cr (99.48 %), Mn (98.26 %), Fe (100 %), Ni (95.93 %), Zn (100 %), As (100 %), Sr (100 %), Zr (99,48 %) and Pb (99,48 %) and Cu (83.2 %). The LODs of the pXRF were calculated as half the minimum quantified (limit of quantification, LOQ) concentration for all samples analysed (Table 2). Finally, for statistical purposes, the concentrations of elements with less than 25 % non-detectable values were adjusted to half the concentration limit of each element (Reimann and Filzmoser, 2000; Zhang et al., 2005).

4. Results and discussion

4.1. Optimisation of calibration method and analysis time

The MLE-FP method can analyse the major elements Mg, Al, Si and P, but it cannot analyse the trace elements V, Cr, Mo, Sn and Sb. However, the S-FP method is able to analyse all elements except the lightest ones (Mg, Al, Si and P). In this study, the MLE-FP method at both 45 s and 90 s has determined an R^2 greater than 0.9 and a RP between 90 and 120 % for Mn, Zr, Th and As (Table 3). The elements Al, K, Ca, Ti, Zn, and Rb show an R^2 between 0.7 and 0.9 and an acceptable RP for the two measurement times, with occasional variations. Other elements that have a high R^2 but an RP higher than 120 % are Mg, P and Pb, while Ba shows a very low RP. There are also elements with a low R^2 and an acceptable RP, such as Si, Cu and Sr. Finally, it should be noted that Fe, Co and Ta have an R^2 lower than 0.43. Furthermore, the S-FP method demonstrated R^2 values greater than 0.9 and a RP range between 80 and 120 for 45 s measurements across a number of elements, including K, Ca, Ti, Cr, Mn, Fe, Ni, Zn, As, Rb, Sr, Zr, Mo, Ba, and Pb. The analysis of Cu at 45 s and Cu and Sr at 90 s obtained an R^2 of 0.7 to 0.9 and a RP range between 80 % to 120 %.

Other studies have found that a 30 s measurement time obtained positive correlations compared to a measurement of 60 s (Silva et al., 2020; Silva et al., 2021). In plant tissues (Sapkota et al., 2019), it has been observed that the increasing measurement time (60, 120 and 180 s) does not significantly affect the correlation with the obtained concentration. In line with these findings, both the MLE-FP and S-FP methods used in this study provide higher R^2 values and reliable RP for the elements Mg, Al, P, K, Ca, Ti, Cr, Mn, Fe, Ni Cu, Zn, As, Rb, Sr, Zr, Mo, Ba, Pb, Th and U using a 45 s measurement time. In this verification, the analytical parameters were optimised in terms of the elements analysed and the analysis time prior to optimising the matrix preparation treatment.

4.2. Optimisation of sample preparation

Verification of the matrix effect, defined as the influence of soil properties on measurement outcomes depending on the sample preparation method (P1: raw; P2: sieved to 2 mm; P3: ground <125 μm; P4: pellet), was analysed using two methods, MLE-FP and S-FP. In the case of MLE-FP, minimum preparations (P1-P3) tend to underestimate Mg and Al but overestimate P, K, Ca, Ti, Cr, Fe, Cu, Zn, As, Rb, Sr, Zr and Pb compared to P4 and the reference analysis (R). In contrast, P4 provides results that are closer to R, with acceptable RP values (85.6–121.9 %) for Mg, Al, K, Ca, Ti, Fe, Zn, As, Rb, Sr, Zr and Zn. For P, the RP is 229.6 and no analyses were performed for Ni, Cr, and Cu. Using the S-FP method, the interquartile range for P1-P3 samples are similar, with an acceptable RP for all elements compared to P4 and R (Fig. 3, Fig. S1 and S2). An underestimation of Cr concentration is observed in the analyses of samples with low preparations (P1-P3), compared to P4 and the reference sample (R) (Fig. S2). In similar studies, accurate pXRF measurements were obtained when compared to benchtop XRF and ICP-MS/OES (AR) (Sarala, 2016; Sarala et al., 2015; Caporale et al., 2018). Regarding sample preparation, the most robust correlations with benchtop XRF were obtained using P4, although P3 samples were also found to be effective (Goff et al., 2020).

Using low-grade preparation type samples (P1-P3), the MLE-FP method did not accurately determine the result with respect to the R samples, although P4 did. Therefore, the validation for Mg, Al, P, K, Ca, Ti, Mn and Fe, and trace elements with these low-grade preparations was unsuccessful. Despite this, the S-FP method, which does not measure Mg, Al and P, provided a favourable analysis, successfully validating the matrix effect for low-grade sample preparations (P1-P3) for K, Ca, Ti, Mn and Fe and trace elements (Cr, Ni, Cu, Zn, As, Rb, Sr, Zr and Pb). K, Ca and Fe, support the study of soil parent material composition (Cicchella et al., 2023). Trace elements, which are considered more sensitive to external influences and produce anomalies in natural variability, can distinguish natural values from those potentially contaminated by anthropogenic factors, even at low concentrations in soils.

Therefore, this methodology can be employed to analyse soils with a low-grade sample preparation with pXRF equipment and the S-FP method. Accordingly, Cuenca province samples were analysed under the minimal preparation protocol (P4). Nevertheless, residual matrix effects, such as mineralogical interferences or element interaction, may still bias the results. Although moisture, humidity and grain size were controlled, matrix correction in portable configurations remains subject to limitations. This approach offers a significant advantage over conventional laboratories, providing the ability to generate geochemical maps of large sample datasets in an efficient timeframe. The methodology also supports many of the 12 principles of green chemistry, including waste prevention, safer chemistry and energy efficiency (Anastas and Warner, 2000; Ivanković, 2017).

4.3. Evaluation of pXRF measurements with the geological context and geochemical atlases of Cuenca province (Spain)

4.3.1. Comparison with European and national programmes

The European FOREGS and GEMAS programmes have only four and seven samples, respectively, in Cuenca province, due to their continental scale and low sampling density (1/4700 km^2 and 1/2500 km^2, respectively). Therefore, the comparison with our SCLM sampling is merely illustrative. The comparison serves to highlight the limitations of these large-scale programmes and to objectify the necessity for regional geochemical studies. Although subject to certain limitations and interpreted in a general sense, the observed geochemical patterns exhibit a coherent and consistent alignment with continental scale geochemical trends (Fig. 4). This correspondence supports the reliability of the SCLM results and reinforces their relevance within a broader geochemical framework. For a robust comparison, the IGME national programme was used. In this case, the sampling density was comparable to that used in this study, with a total of 162 samples, providing a representative statistical comparison.

In these programmes, the presence of upper and lower outliers is high. There is an extreme Zn outlier in a sample from the IGME campaign, and it should be noted that the existing limitation in the analysis of Sr with a limit of quantification higher than 1000 mg kg^{-1} does not permit observing the presence of higher values as observed in the other programmes. Despite these differences, the overall results are comparable (IGME vs SCLM) even though different analytical techniques (XRF, ICP-MS, ICP-AES, INAA and pXRF) were used. Results show similar and comparable interquartile ranges, except for Ti and Zr. Beyond the analytical techniques employed, other factors that may account for these variations include sampling distribution, geochemical change over the ten-year period between the different campaigns,

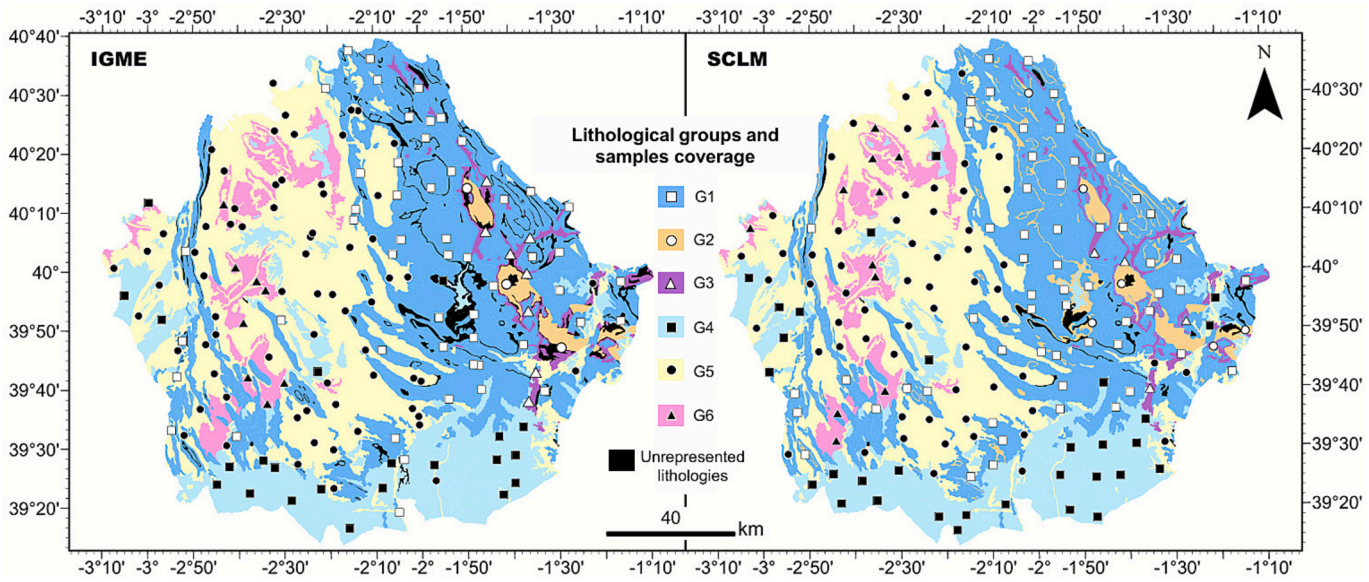

Fig. 5. Map of the IGME and SCLM sampling programmes. The map displays the symbology of the samples classified into the six established lithological groups (G1-G6), overlaid on a simplified geological background. This background was derived from the Geological Maps of Spain (1:1,000,000 scale). Lithologies not represented by the sampling are shown in black.

Table 4
Extension and representativity estimations of the IGME and SCLM campaign. LG: lithological group. RI: representativeness index.

LG	Area standardisation (%)	IGME samples	Samples in each LG (%)	RI	Area standardisation (%)	SCLM samples	Samples in each LG (%)	RI
G1	35.74	52	32.10	0.90	35.42	58	33.53	0.96
G2	1.74	3	1.85	1.07	4.09	6	3.47	0.86
G3	2.08	8	4.94	2.38	2.01	4	2.31	1.16
G4	19.19	22	13.58	0.71	18.54	30	17.92	0.98
G5	35.63	69	42.59	1.20	34.50	62	35.84	1.05
G6	5.63	8	4.94	0.88	5.45	12	6.94	1.29

climate, soil, and anthropogenic processes.

4.3.2. *Limitations and representativeness of sampling strategies*

Sampling design and strategy directly impact the geochemical representativeness (Reimann and Garrett, 2005).Variations in sampling density, soil cover use or incomplete lithological representation led to partial or asymmetric interpretations of the natural geochemistry of an area. In large-scale projects, such as national programmes, these limitations are caused by the type of strategy adopted in the sampling campaign and due to logistical difficulties or lack of accessibility of certain environments, which results in deficiencies in capturing the geochemical heterogeneity of a site. This leads to underrepresentation of key lithologies and limits the reliability of spatial extrapolations and statistical comparisons, including the calculation of GB.

To verify the representativeness of SCLM and IGME campaigns against the geology of Cuenca province (covering 17,127 km^2), a spatial analysis of the percentage of occupation of each lithological group was performed with the geological map of Spain at 1:1,000,000 scale. Based on generalisations and simplifications of the province's geology, six lithological groups of parent materials were defined for the soil samples (Fig. 5, classified in section 2). It's noteworthy that the Variscan Massif domain, comprising an area of 26 km^2 (0.15 % of Cuenca province), is not represented in any of the programmes. The SCLM campaign (n = 173) successfully represents 98.96 % of the existing lithologies. In contrast, the IGME campaign (n = 162) shows a lower representation at 95.63 % of the lithologies. Areas not represented by either campaign are marked with black polygons (Fig. 5).

Regarding AB Domain, lithological groups G1 and G2 show similar RI between the different geochemical campaigns (Table 4). However, for group G3, the RI obtained by the IGME programme is significantly higher, by a factor of 2, compared to the SCLM RI (2.36 and 1.16, respectively). In the QCCB Domain, G4 is underrepresented by the IGME campaign. Meanwhile, G6 shows contrasting results: it is over-represented by the SCLM but underrepresented by the IGME. The overrepresentation in the SCLM campaign effectively highlights the different evaporitic, gypsum-rich deposits across the various sub-basins of the QCCB Domain. The distribution of the SCLM samples shows a greater homogeneity associated with the regular systemic strategy applied, compared to the IGME sampling (Fig. 5). The strategy employed by IGME produces sampling gaps that are observed at different points in Cuenca province. For example, although G6 are represented by different samples, the deposits in the centre of the Intermediate Depression, the north of the Madrid Basin and the west of the La Mancha Plain are not represented. Another setting where large areas lack samples is in the southeast of the province, on the border of the AB and in QCCB domains.

Regarding the complete representation of the geological structures within the province, both the SCLM and the IGME campaigns exhibit a misrepresentation of the Altomira Mountain Range. The narrowness of this landscape makes it difficult to represent it with the density and sampling strategy employed. The presence of folded structures, stratigraphically discordant deposits or superficial deposits and narrow, small and elongated outcrops, such as Altomira Mountain Range or the outcrops of the IVB Domain, represent other complex geological areas that hinder a correct representation in national and regional campaigns. It should be noted that another limitation in this analysis is the existing polygonal simplification of large-scale geology (1:1,000,000 scale). These results imply that the existence of data gaps, over- and under-representations, and the complexity of regional geological settings all

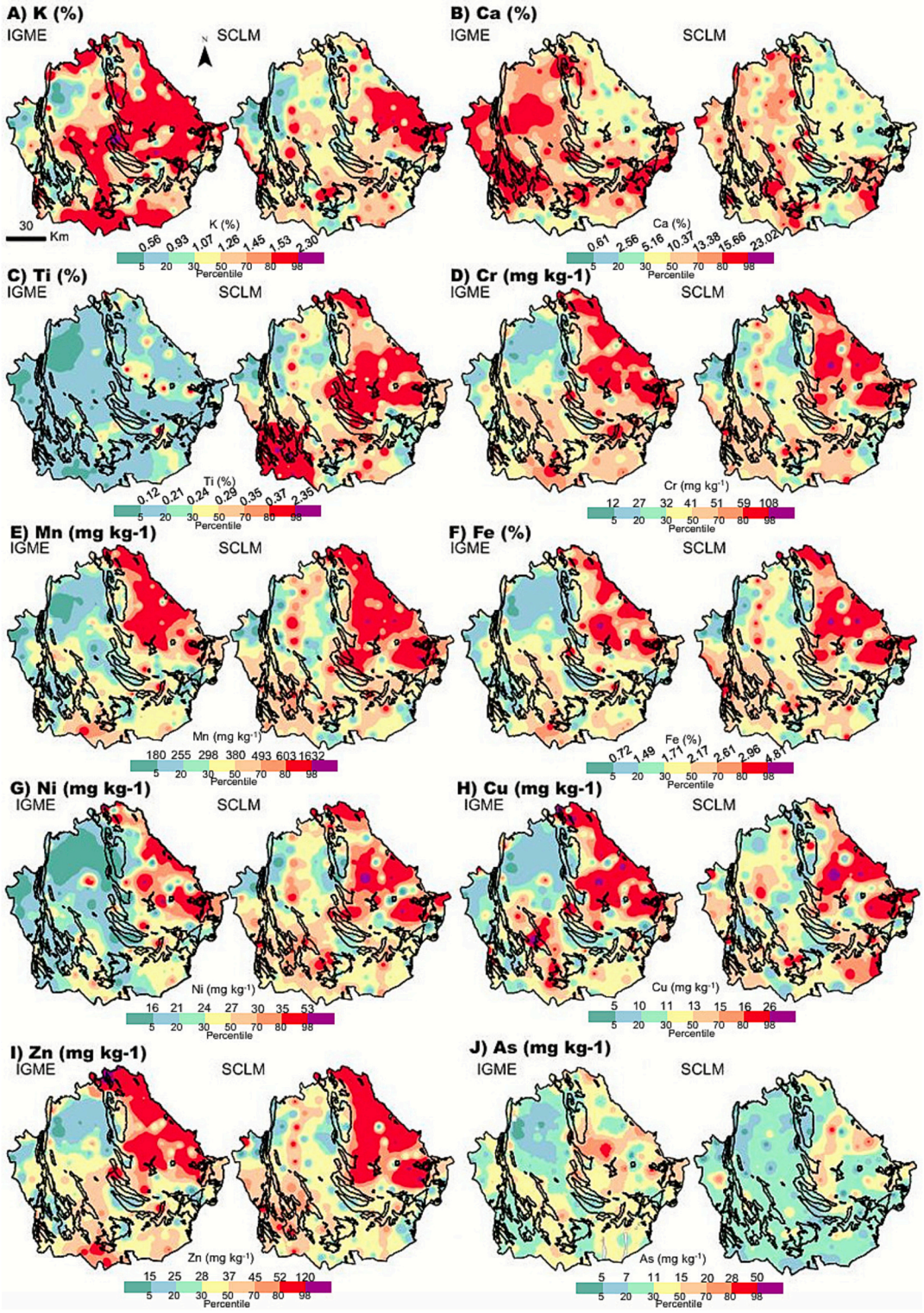

Fig. 6. Spatial distribution maps of K, Ca, Ti, Cr, Mn, Fe, Ni, Cu, Zn, and As in surface soil of Cuenca province. The figure compares results from the SCLM study (this work) with the IGME programme (modified from Locutura Rupérez et al., 2012). Percentiles for visualization were calculated using the SCLM data for all elements, except for As, which was based on the IGME data.

give rise to varying degrees of uncertainty. This uncertainty can be mitigated with a sampling design strategy that takes these aspects into account. These variables can modify the geochemical patterns of a setting, thereby distorting the calculation of GB. Although machine learning techniques are not suitable for directly establishing GBs, their application can be useful for enhancing the representation of geochemical variability and reducing the uncertainty associated with sampling scale and geological heterogeneity (Azizi et al., 2022; Hu et al., 2025; Wilford et al., 2016).

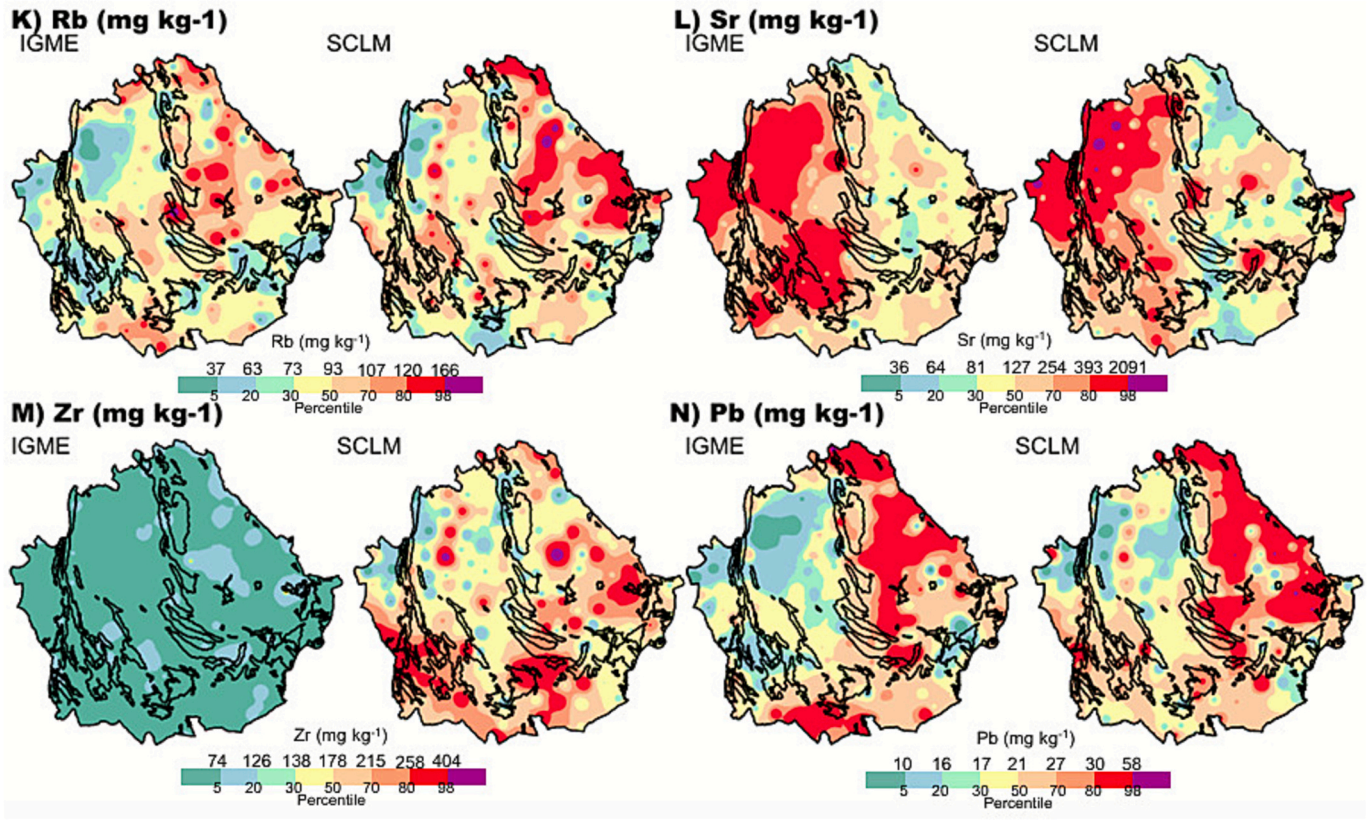

Fig. 7. Spatial distribution maps of Rb, Sr, Zr and Pb in surface soil of Cuenca province. The figure compares results from the SCLM study (this work) with the IGME programme (modified from Locutura Rupérez et al., 2012).

4.3.3. Regional geochemical patterns and comparative analysis with IGME dataset

The spatial distribution maps presented in this study closely resemble those produced by the IGME for the elements K, Ca, Mn and Fe, as well as for the trace elements (Cr, Ni, Cu, Zn, As, Rb, Sr, and Pb). In general terms, the geochemical patterns observed in this study are similar to those reported by the IGME (Figs. 6 and 7). However, a significant contrast exists in the Intermediate Depression (located northwest of Cuenca province, between the Altomira Mountain Range and Cuenca Mountain Range). Here, the IGME programme identifies a depletion zone for Ti, Mn and Fe and trace elements, a pattern that is notably disrupted in SCLM maps by elevated concentrations. This discrepancy is directly linked to the fact that the IGME sampling failed to include the Paleogene-Neogene gypsiferous deposits in this specific area. These deposits, whose derived parent materials are responsible for the higher concentrations in the SCLM samples, account for the observed difference. Finally, the patterns for Ca are reversed (SCLM shows lower concentrations, IGME shows higher ones), with the IGME programme generally reporting higher concentrations, as reflected in the interquartile ranges (Fig. 4).

In contrast, the elements K, Ti, and Zr exhibit the greatest discrepancies between the two programmes (Figs. 6 and 7). Specifically for Ti and Zr, the interquartile ranges in our study are shifted towards higher values compared to those obtained in the IGME dataset (Fig. 4). The comparable sampling density of 1/100 km^2 across Cuenca province enables a more detailed comparison with SCLM study. The distribution maps from both programmes reveal regional geochemical patterns, with local variations attributable to differing sampling strategies, and broader regional differences linked to the distinct analytical techniques employed.

4.3.4. Geochemical signatures and spatial distribution of analysed soil samples

Based on the results obtained in this study, distinct groups of elements can be identified according to their geochemical distribution patterns, indicating the influence of the parent rock on which the soils studied have developed. A major group, comprising Ti, Cr, Mn, Fe, Ni, Zn, Rb, Zr, Pb and As, exhibits similar spatial behaviour, though Mn, Zn and Pb show more uniformed trends (Figs. 6 and 7). In contrast, other elements, such as K, Ca, and Sr, show independent distribution patterns.

The disparities observed in the Mn, Zn, and Pb with respect to the first group reflect a heightened degree of variability in geochemical patterns within the AB Domain. This variability is attributed to soil development over detrital parent materials with low elemental concentrations. The elevated concentrations in the AB Domain originated primary from G1 and G3 in the Cuenca Mountain Range, followed by G4 and G6 in the Intermediate Depression, the Madrid Basin, and the La Mancha Plain within the QCCB Domain (Fig. 8). For K, the highest concentrations are also located in the AB Domain, particularly in G3 and its surrounding area, which is bordered by G2 and G3. In contrast, Ca displays geochemical patterns with higher concentrations in the QCCB Domain, across the various lithologies that compose it. Sr similarly shows its highest concentrations within the QCCB Domain, with a notable focus in G6 and adjacent areas. The predominance of Sr anomalies in Spain is associated with Neogene basins filled by chemical and evaporitic sedimentary materials, including limestone, gypsum, and anhydrite. These formations are characteristic of regions such as the Duero and Tajo basins and the La Mancha Plain, where extensive gypsum deposits are presented (Locutura Rupérez et al., 2012).

Compared to previous research conducted in Cuenca province, this study provides a more detailed spatial resolution and more accurate representation of soil diversity. For example, (Bravo et al., 2019) presented data based on a very low sampling density of approximately 30

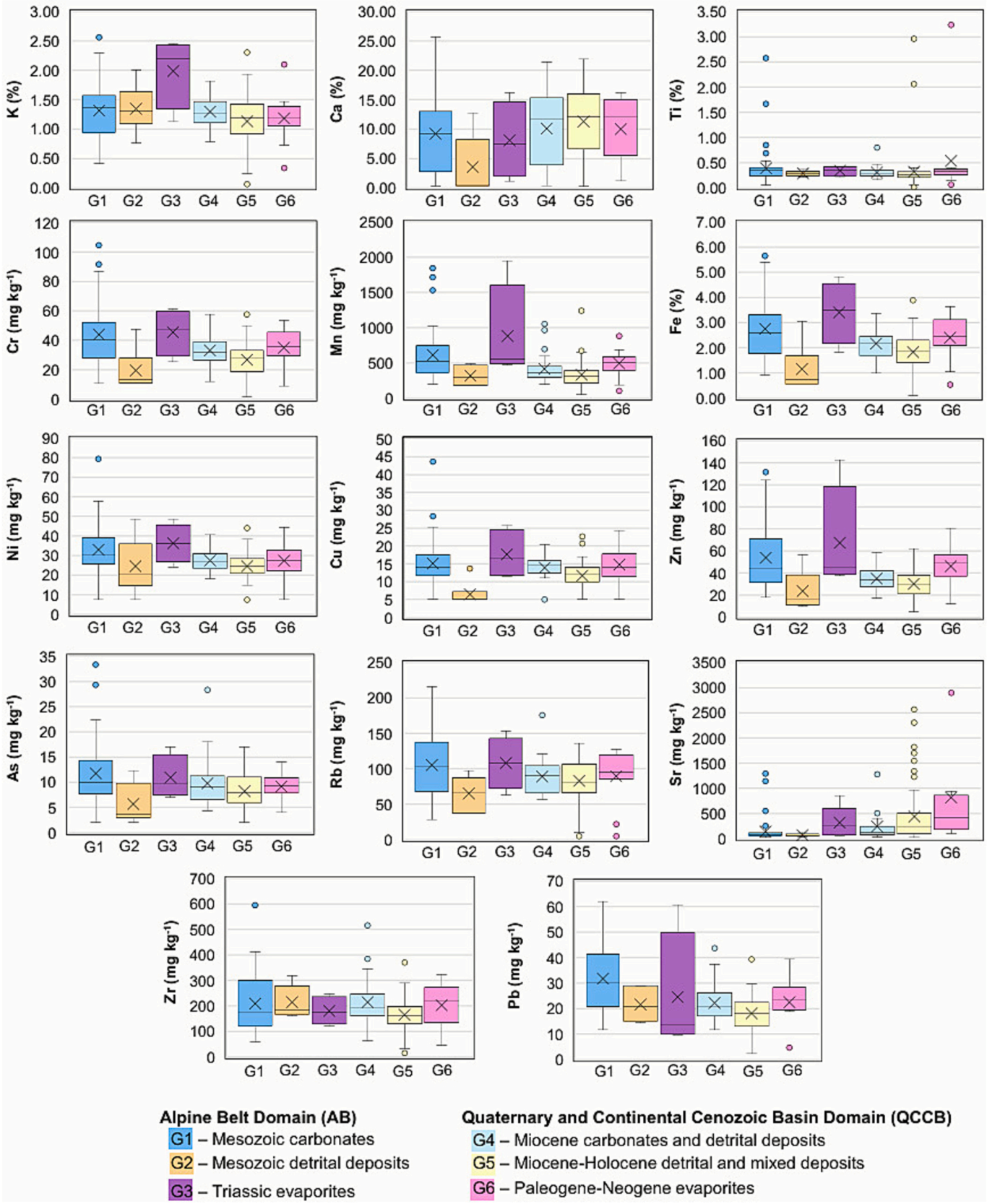

Fig. 8. Boxplots showing the variation of the content of the selected elements in the six lithological groups. Groups G1 ($n = 58$), G2 ($n = 6$) and G3 ($n = 4$) are part of the AB domain and G4 ($n = 30$), G5 ($n = 62$) and G6 ($n = 12$) are part of the QCCB domain.

samples across the entire province. Their sampling strategy lacked a criterion for spatial representativeness, and the distribution of sampling locations was non-uniform. Consequently, the representativeness of soils derived from parent rocks in Cuenca province was limited. Additionally, their dataset, which includes 200 samples for the entire Castilla-La Mancha region, did not offer sufficient detail to accurately calculate GB and reference values, which could lead to inaccurate results. Another study (Ballesta et al., 2010), also estimated GB and reference values based on only 24 sample points for Castilla-La Mancha, of which just two were from Cuenca province, which introduces even greater uncertainty.

The results obtained from the SCLM campaign provide a more detailed understanding of the geochemical nature of Cuenca province. Following the proposed methodology, which utilises pXRF and low-grade sample preparation, the GB can be calculated without the uncertainties introduced by poor sampling strategies, making the data suitable for future environmental and geochemical exploration studies. The incorporation of machine learning could further improve the interpolations by addressing the existing problems observed in the geological variables, especially when combined with the use of geological maps of higher resolution (e.g., 1:50,000 scale).

5. Conclusions

The verification of pXRF equipment for soils analysis is of vital importance, as its performance plays an important role regardless of the use of FP methods or the internal software of the equipment designed for matrix correction. The optimisation of the method established 45 s as the optimal measurement time, balancing analytical quality with equipment longevity. This time yielded a high and acceptable Recovery Percentage (RP) for a wide range of elements: Mg, Al, P, and Th using the MLE-FP method, and K, Ti, Ni, Cu, Zn, As, Rb, Sr, Zr, Mo, Ba, Pb, and U using the S-FP method. In terms of sample preparation, low-grade preparation (P1-P3) were unreliable with MLE-FP method. However, the S-FP method successfully achieved acceptable RPs for K, Ca, Ti, Cr, Mn, Fe, Ni, Cu, Zn, As, Rb, Sr, Zr and Pb, validating its robustness even with minimal sample treatment.

The optimised S-FP methodology was successfully applied to 173 soil samples from the SCLM project in Cuenca province. It was demonstrated that European continental patterns (FOREGS and GEMAS programmes) are consistent with the results of this study, although the comparison is merely illustrative due to the low sampling density. However, with the national programme of the Geochemical Atlas of Spain (IGME), the comparison is statistically robust, given its equivalent sampling density (1/100 km^2). Similarities in the interquartile ranges and regional geochemical patterns are evident for K, Ca, Cr, Mn, Fe, Ni, Cu, Zn, Rb, As, Sr and Pb, except for Ti and Zr. The recognition of varying local geochemical patterns suggests a methodological influence, highlighting differences emerging between results obtained via ICP-MS, ICP-AES, and INAA versus those from pXRF.

The samples analysed in this study exhibit distinct geochemical patterns. Overall, Ti, Mn, Fe and trace elements (excluding Sr) show elevated concentrations within the AB Domain, particularly in G1 (Mesozoic carbonates), G2 (Triassic evaporites) and G6 (Paleogene-Neogene gypsum deposits) of the QCCB Domain. In contrast, K achieves its highest concentrations in G3 and adjacent soils. With respect to Ca, generally dominates the QCCB domain. As for Sr, has its highest concentration in Intermediate Depression and Madrid Basin of Cuenca province.

This study also addresses a common challenge in large geographic regions: the lack of geochemical characterization resulting from the high cost of conventional laboratory analyses. In Castilla-La Mancha, the suspension of the SCLM project for budgetary reasons has prevented the completion of its geochemical atlas, a barrier directly linked to the expense of traditional analytical methods. In this context, pXRF emerges as a rapid, cost-effective, and environmentally friendly alternative to bridge this analytical gap. Following this methodology, a geochemical atlas of Castilla-La Mancha could be created, and the geochemical background calculated. Furthermore, this approach supports the development of standardised protocols for the analysis of soils across a wide range of parameters, including nutrients, potential toxic elements (PTEs) or Critical Raw Materials such as rare earth elements.

CRediT authorship contribution statement

Iker Martínez-del-Pozo: Writing – review & editing, Writing – original draft, Visualization, Validation, Software, Methodology, Investigation, Formal analysis, Data curation, Conceptualization. **Mónica Celina Gómez-Pachón:** Investigation, Formal analysis. **Inmaculada Ferri-Moreno:** Writing – review & editing, Investigation. **Mari Luz García-Lorenzo:** Writing – review & editing, Supervision, Funding acquisition. **Saturnino Lorenzo:** Investigation, Conceptualization. **José Ignacio Barquero-Peralbo:** Investigation. **Xabier Arroyo:** Investigation. **Pablo Higueras:** Funding acquisition, Conceptualization. **José María Esbrí:** Writing – review & editing, Validation, Supervision, Resources, Project administration, Funding acquisition, Data curation, Conceptualization.

Declaration of competing interest

The authors declare that they have no known competing financial interests or personal relationships that could have appeared to influence the work reported in this paper.

Acknowledgements

This work was funded by the project “Biogeoquímica de suelos de Castilla-La Mancha – Elaboración de mapas temáticos y establecimiento de niveles de base y de referencia”, reference SBPLY/17/180501/000273/1, IP Pablo Higueras and supported by the Spanish “Ministerio de Ciencias e Innovación” (reference project: TED2021-130498B-I00).

The authors are grateful for the use of the geochemical documentation available in the database of the following European Union initiatives, which were essential for the analysis in this study: FOREGS (Forum of European Geological Surveys), GEMAS (Geochemical Mapping of Agricultural and Grazing Land Soil), LUCAS (Land use/Cover Area Frame Survey) and the IGME Geochemical Atlas of Spain.

Appendix A. Supplementary data

Supplementary data to this article can be found online at https://doi.org/10.1016/j.gexplo.2025.107961.

Data availability

Data will be made available on request.

References

Alonso-Zarza, A.M., Calvo, J.P., Silva, P.G., Torres, T., 2004. Cuenca del Tajo. In: Vera, J. A. (Ed.), Geología de España. SGE-IGME, Madrid, pp. 556–561.

Anastas, P.T., Warner, J.C., 2000. Green Chemistry. Oxford University Press, Oxford. https://doi.org/10.1093/oso/9780198506980.001.0001.

Arribas, J., Díaz-Molina, M., 1996. Saline deposits associated with fluvial fans, Late Oligocene–Early Miocene, Loranca Basin, Central Spain. In: Friend, P., Dabrio, C. (Eds.), Tertiary Basins of Spain. Cambridge University Press, Cambridge, pp. 308–312.

Azizi, K., Ayoubi, S., Nabiollahi, K., Garosi, Y., Gislum, R., 2022. Predicting heavy metal contents by applying machine learning approaches and environmental covariates in west of Iran. J. Geochem. Explor. 233. https://doi.org/10.1016/j.gexplo.2021.106921.

Ballesta, R., Bueno, P., Rubí, J., Giménez, R., 2010. Pedo-geochemical baseline content levels and soil quality reference values of trace elements in soils from the Mediterranean (Castilla la Mancha, Spain). Cent. Eur. J. Geosci. 2, 441–454. https://doi.org/10.2478/v10085-010-0028-1.

Bednářová, Z., Kalina, J., Hájek, O., Sáňka, M., Komprdová, K., 2016. Spatial distribution and risk assessment of metals in agricultural soils. Geoderma 284, 113–121. https://doi.org/10.1016/j.geoderma.2016.08.021.

Bölviken, B., Bogen, J., Demetriades, A., De Vos, W., Ebbing, J., Hindel, R., et al., 1996. Regional geochemical mapping of Western Europe towards the year 2000. J. Geochem. Explor. 56, 141–166. https://doi.org/10.1016/0375-6742(96)00025-8.

Borges, C.S., Weindorf, D.C., Nascimento, D.C., Curi, N., Guilherme, L.R.G., Carvalho, G. S., et al., 2020. Comparison of portable X-ray fluorescence spectrometry and laboratory-based methods to assess the soil elemental composition: applications for wetland soils. Environ. Technol. Innov. 19. https://doi.org/10.1016/j.eti.2020.100826.

Bravo, S., García-Ordiales, E., García-Navarro, F.J., Amorós, J.Á., Pérez-de-los-Reyes, C., Jiménez-Ballesta, R., et al., 2019. Geochemical distribution of major and trace elements in agricultural soils of Castilla-La Mancha (central Spain): finding criteria for baselines and delimiting regional anomalies. Environ. Sci. Pollut. Res. 26, 3100–3114. https://doi.org/10.1007/s11356-017-0010-6.

Bustos, N., Marquardt, C., Belmar, Á., Cordeiro, P., 2022. Regolith-hosted rare earth exploration in the Chilean Coastal Range of the Central Andes. J. Geochem. Explor. 234. https://doi.org/10.1016/j.gexplo.2021.106934.

Byers, H.L., McHenry, L.J., Grundl, T.J., 2016. Forty-nine major and trace element concentrations measured in soil reference materials NIST SRM 2586, 2587, 2709a, 2710a and 2711a Using ICP-MS and wavelength dispersive-XRF. Geostand. Geoanal. Res. 40, 433–445. https://doi.org/10.1111/j.1751-908X.2016.00376.x.

Calvo, J.P., Zarza, A.M.A., Cura, M.A.G. Del, Ordóñez, S., Rodríguez-Aranda, J.P., Montero, M.E.S., 1996. Sedimentary evolution of lake systems through the Miocene of the Madrid Basin: paleoclimatic and paleohydrological constraints. In: Tertiary Basins of Spain. Cambridge University Press, pp. 272–277. https://doi.org/10.1017/CBO9780511524851.038.

Caporale, A.G., Adamo, P., Capozzi, F., Langella, G., Terribile, F., Vingiani, S., 2018. Monitoring metal pollution in soils using portable-XRF and conventional laboratory-based techniques: evaluation of the performance and limitations according to metal properties and sources. Sci. Total Environ. 643, 516–526. https://doi.org/10.1016/j.scitotenv.2018.06.178.

de Caritat, P. de, Reimann, C., Smith, D.B., Wang, X., 2018. Chemical elements in the environment: multi-element geochemical datasets from continental- to national-scale surveys on four continents. Appl. Geochem. 89, 150–159. https://doi.org/10.1016/j.apgeochem.2017.11.010.

Cheng, Z., Xie, X., Yao, W., Feng, J., Zhang, Q., Fang, J., 2014. Multi-element geochemical mapping in Southern China. J. Geochem. Explor. 139, 183–192. https://doi.org/10.1016/j.gexplo.2013.06.003.

Cicchella, D., Ambrosino, M., Albanese, S., Guarino, A., Lima, A., De Vivo, B., et al., 2023. Major elements concentration in soils. A case study from Campania Region (Italy). J. Geochem. Explor. 247. https://doi.org/10.1016/j.gexplo.2023.107179.

Escavy, J.I., Herrero, M.J., Arribas, M.E., 2012. Gypsum resources of Spain: temporal and spatial distribution. Ore Geol. Rev. 49, 72–84. https://doi.org/10.1016/j.oregeorev.2012.09.001.

European Commission, 2024. REGULATION (EU) 2021/1058 OF THE EUROPEAN PARLIAMENT AND OF THE COUNCIL of 24 June 2021 on the European Regional Development Fund and on the Cohesion Fund of the European Parliament and of the Council of 11 December 2013 on Union Guidelines for the Development of the Trans-European Transport Network and Repealing Decision. Brussels.

Fedeli, R., Di Lella, L.A., Loppi, S., 2024. Suitability of XRF for routine analysis of multi-elemental composition: a multi-standard verification. Methods Protoc. 7, 53. https://doi.org/10.3390/mps7040053.

Gałuszka, A., Migaszewski, Z., 2011. Geochemical background-an environmental perspective. Mineralogia 42. https://doi.org/10.2478/v10002-011-0002-y.

Gobierno de España, 2005. Real Decreto 9/2005, de 14 de enero, por el que se establece la relación de actividades potencialmente contaminantes del suelo y los criterios y estándares para la declaración de suelos contaminados. Madrid.

Goff, K., Schaetzl, R.J., Chakraborty, S., Weindorf, D.C., Kasmerchak, C., Bettis, E.A., 2020. Impact of sample preparation methods for characterizing the geochemistry of soils and sediments by portable X-ray fluorescence. Soil Sci. Soc. Am. J. 84, 131–143. https://doi.org/10.1002/saj2.20004.

Haschke, M., Flock, J., Haller, M., 2021. X-ray Fluorescence Spectroscopy for Laboratory Applications. https://doi.org/10.1002/9783527816637.

Horta, A., Malone, B., Stockmann, U., Minasny, B., Bishop, T.F.A., McBratney, A.B., et al., 2015. Potential of integrated field spectroscopy and spatial analysis for enhanced assessment of soil contamination: a prospective review. Geoderma 241, 180–209. https://doi.org/10.1016/j.geoderma.2014.11.024.

Hu, H., Zhou, W., Liu, X., Guo, G., He, Y., Zhu, L., et al., 2025. Machine learning combined with geodetector to predict the spatial distribution of soil heavy metals in mining areas. Sci. Total Environ. 959. https://doi.org/10.1016/j.scitotenv.2024.178281.

Ivanković, A., 2017. Review of 12 principles of green chemistry in practice. Int. J. Sustain. Green Energy 6, 39. https://doi.org/10.11648/j.ijrse.20170603.12.

Kazimoto, E.O., Messo, C., Magidanga, F., Bundala, E., 2018. The use of portable X-ray spectrometer in monitoring anthropogenic toxic metals pollution in soils and sediments of urban environment of Dar es Salaam Tanzania. J. Geochem. Explor. 186, 100–113. https://doi.org/10.1016/j.gexplo.2017.11.016.

Lemière, B., 2018. A review of pXRF (field portable X-ray fluorescence) applications for applied geochemistry. J. Geochem. Explor. 188, 350–363. https://doi.org/10.1016/j.gexplo.2018.02.006.

Li, S., Shen, J., Bishop, T.F.A., Viscarra Rossel, R.A., 2022. Assessment of the effect of soil sample preparation, water content and excitation time on proximal X-ray fluorescence sensing. Sensors 22, 4572. https://doi.org/10.3390/s22124572.

Locutura Rupérez, J., Bel-Lan, A., García Cortés, A., Martínez, S., 2012. Atlas geoquímico de España. Consejo Superior de Investigaciones Científicas, Publicación del IGME, Madrid.

McNulty, B.A., Fox, N., Berry, R.F., Gemmell, J.B., 2018. Lithological discrimination of altered volcanic rocks based on systematic portable X-ray fluorescence analysis of drill core at the Myra Falls VHMS deposit, Canada. J. Geochem. Explor. 193, 1–21. https://doi.org/10.1016/j.gexplo.2018.06.005.

Plotts, P.J., Tindle, A.G., Webb, P.C., 1992. Geochemical Reference Material Composition: Rocks, Minerals, Sediments, Soils, Carbonates, Refractories & Ores Used in Research and Industry, vol. 551.9. Whittles Publishing, UK.

Reimann, C., Filzmoser, P., 2000. Normal and lognormal data distribution in geochemistry: death of a myth. Consequences for the statistical treatment of geochemical and environmental data. Environ. Geol. 39, 1001–1014. https://doi.org/10.1007/s002549900081.

Reimann, C., Garrett, R.G., 2005. Geochemical background - concept and reality. Sci. Total Environ. 350, 12–27. https://doi.org/10.1016/j.scitotenv.2005.01.047.

Reimann, C., Demetriades, A., Eggen, O.A., Filzmoser, P., The EuroGeoSurveys Geochemical Expert Group, 2009. The EuroGeoSurveys Geoeochemical Mapping of Agricultural and Grazing Land Soils Project (GEMAS) -Evaluation of Quality Control Results of Aqua Regia Extraction Analysis, 049. Geological Survey of Norway, Trondheim, p. 94. NGU Report.

Reimann, C., Demetriades, A., Eggen, O.A., Filzmoser, P., The EuroGeoSurveys Geochemistry Expert Group, 2011. The EuroGeoSurveys Geochemical Mapping of Agricultural and Grazing Land Soils Project (GEMAS) – Evaluation of Quality Control Results of Total C and S, Total Organic Carbon (TOC), Cation Exchange Capacity (CEC), XRF, pH, and Particle Size Distribution (PSD) Analysis, 043. Geological Survey of Norwey, Trondheim, p. 92. NGU Report.

Rodríguez Fernández, L.P., López Olmedo, F., Oliveira, J.T., Medialdea, T., Terrinha, P., Matas, J., et al., 2015. Mapa Geológico de España y Portugal, escala 1:1.000.000. IGME-LNEG.

Ross, P.S., Beaudette, M., Daoudene, Y., 2024. Portable XRF applied to regional bedrock mapping in Quebec, Canada. J. Geochem. Explor. 258. https://doi.org/10.1016/j.gexplo.2024.107397.

Salminen, R., Batista, M.J., Bidovec, M., Demetriades, A., De Vivo, B., De Vos, W., Duris, M., Gilucis, A., Gregorauskiene, V., Halanic, J., Heitzmann, P., Lima, A., Jordan, G., Klaver, P., Lis, J., Locutura, J., Marsina, K., Mazreku, A., O'Connor, P.J., Olsson, S.A., Ottesen, R.T., Petersell, V., Plant, J.A., Reeder, S., Salpeteur, I., Sanström, H., Siewers, U., Steenfelt, A., Tarvainen, T., 1998. Geochemical Atlas of Europe. Part 1. Background information, methodology and maps. Geological Survey of Finland.

Sapkota, Y., McDonald, L.M., Griggs, T.C., Basden, T.J., Drake, B.L., 2019. Portable X-Ray fluorescence spectroscopy for rapid and cost-effective determination of elemental composition of ground forage. Front. Plant Sci. 10, 317. https://doi.org/10.3389/fpls.2019.00317.

Sarala, P., 2016. Comparison of different portable XRF methods for determining till geochemistry. Geochem.: Explor., Environ., Anal. 16, 181–192. https://doi.org/10.1144/geochem2012-162.

Sarala, P., Taivalkoski, A., Valkama, J., 2015. Portable XRF: an advanced on-site analysis method in till geochemical exploration. Geol. Surv. Finland Spec. Pap. 57, 63–86.

Silva, S.H.G., Weindorf, D.C., Pinto, L.C., Faria, W.M., Acerbi Junior, F.W., Gomide, L.R., et al., 2020. Soil texture prediction in tropical soils: a portable X-ray fluorescence spectrometry approach. Geoderma 362, 11413. https://doi.org/10.1016/j.geoderma.2019.114136.

Silva, S.H.G., Ribeiro, B.T., Guerra, M.B.B., de Carvalho, H.W.P., Lopes, G., Carvalho, G. S., et al., 2021. pXRF in tropical soils: methodology, applications, achievements and challenges. In: Adv. Agron., 167, pp. 1–62. https://doi.org/10.1016/bs.agron.2020.12.001.

Sopeña, A., Gutiérrez-Marco, J.C., De Vicente, G., Sánchez, 2004. Cordilleras Ibérica y Costero-Catalana. In: Geología de España. SGE-IGME, Madrid, pp. 467–527.

Tóth, G., Jones, A., Montanarella, L., 2013. The LUCAS topsoil database and derived information on the regional variability of cropland topsoil properties in the European Union. Environ. Monit. Assess. 185, 7409–7425. https://doi.org/10.1007/s10661-013-3109-3.

Tóth, G., Hermann, T., Da Silva, M.R., Montanarella, L., 2016. Heavy metals in agricultural soils of the European Union with implications for food safety. Environ. Int. 88, 299–309. https://doi.org/10.1016/j.envint.2015.12.017.

United Nations, 2015. Transforming Our World: The 2030 Agenda for Sustainable Development. New York.

Weindorf, D.C., Bakr, N., Zhu, Y., 2014. Advances in portable X-ray fluorescence (PXRF) for environmental, pedological, and agronomic applications. Adv. Agron. 128, 1–45. https://doi.org/10.1016/B978-0-12-802139-2.00001-9.

Wilford, J., de Caritat, P., Bui, E., 2016. Predictive geochemical mapping using environmental correlation. Appl. Geochem. 66, 275–288. https://doi.org/10.1016/j.apgeochem.2015.08.012.

Williams, R., Taylor, G., Orr, C., 2020. pXRF method development for elemental analysis of archaeological soil. Archaeometry 62. https://doi.org/10.1111/arcm.12583.

Yuan, G.L., Sun, T.H., Han, P., Li, J., 2013. Environmental geochemical mapping and multivariate geostatistical analysis of heavy metals in topsoils of a closed steel smelter: Capital Iron & Steel Factory, Beijing, China. J. Geochem. Explor. 130, 15–21. https://doi.org/10.1016/j.gexplo.2013.02.010.

Yuan, Z., Chang, H., Zhou, S., Zhang, Z., Cheng, Q., Xia, Q., et al., 2021. In situ monitoring of elemental losses and gains during weathering using the spatial

element patterns obtained by portable XRF. J. Geochem. Explor. 229. https://doi.org/10.1016/j.gexplo.2021.106842.
Zhang, C., Manheim, F.T., Hinde, J., Grossman, J.N., 2005. Statistical characterization of a large geochemical database and effect of sample size. Appl. Geochem. 20, 1857–1874. https://doi.org/10.1016/j.apgeochem.2005.06.006.
Zhou, S., Cheng, Q., Weindorf, D.C., Yang, B., Gong., Zebin, Yuan, Z., 2024. Multiple approaches for heavy metal contamination characterization and source identification of farmland soils in a metal mine impacted area. Appl. Geochem. 174, 106125. https://doi.org/10.1016/j.apgeochem.2024.106125.